The Journal of Eukaryotic Microbiology

ISOP Published by the International Society of Protistologists

Journal of Eukaryotic Microbiology ISSN 1066-5234

ORIGINAL ARTICLE

Abundant Chitinous Structures in *Chilostomella* (Foraminifera, Rhizaria) and Their Potential Functions

Hidetaka Nomaki*[a], Chong Chen[a], Kaya Oda[a], Masashi Tsuchiya[b], Akihiro Tame[c], Katsuyuki Uematsu[c] & Noriyuki Isobe[d]

a SUGAR, X-star, Japan Agency for Marine-Earth Science and Technology (JAMSTEC), 2-15 Natsushima-cho, Yokosuka, Kanagawa, 237-0061, Japan

b Research Institute for Global Change (RIGC), Japan Agency for Marine-Earth Science and Technology (JAMSTEC), Yokosuka, Kanagawa, 237-0061, Japan

c Marine Works Japan Ltd., 3-54-1 Oppamahigashi-cho, Yokosuka, Kanagawa, 237-0063, Japan

d Research Institute for Marine Resources Utilization (MRU), Japan Agency for Marine-Earth Science and Technology (JAMSTEC), Yokosuka, Kanagawa, 237-0061, Japan

Keywords

3D reconstruction; chitin; cytoplasm; hypoxic adaptation; ultrastructure.

***Correspondence**

Hidetaka Nomaki, SUGAR, X-star, Japan Agency for Marine-Earth Science and Technology (JAMSTEC), 2-15 Natsushima-cho, Yokosuka, Kanagawa 237-0061, Japan

Telephone number: +81-46-867-9795;

Fax number: +81-46-867-9775,

e-mail: nomakih@jamstec.go.jp

Received: 14 June 2020; revised 28 August 2020; accepted October 20, 2020.

Early View publication 20 November, 2020

doi:10.1111/jeu.12828

ABSTRACT

Benthic foraminifera, members of Rhizaria, inhabit a broad range of marine environments and are particularly common in hypoxic sediments. The biology of benthic foraminifera is key to understanding benthic ecosystems and relevant biogeochemical cycles, especially in hypoxic environments. *Chilostomella* is a foraminiferal genus commonly found in hypoxic deep-sea sediments and has poorly understood ecological characteristics. For example, the carbon isotopic compositions of their lipids are substantially different from other co-occurring genera, probably reflecting unique features of its metabolism. Here, we investigated the cytoplasmic and ultrastructural features of *Chilostomella ovoidea* from bathyal sediments of Sagami Bay, Japan, based on serial semithin sections examined using an optical microscope followed by a three-dimensional reconstruction, combined with TEM observations of ultra-thin sections. Observations by TEM revealed the presence of abundant electron-dense structures dividing the cytoplasm. Based on histochemical staining, these structures are shown to be composed of chitin. Our 3D reconstruction revealed chitinous structures in the final seven chambers. These exhibited a plate-like morphology in the final chambers but became rolled up in earlier chambers (toward the proloculus). These chitinous, plate-like structures may function to partition the cytoplasm in a chamber to increase the surface/volume ratio and/or act as a reactive site for some metabolic functions.

BENTHIC foraminifera, members of Rhizaria, are abundant constituents of marine ecosystems. Their habitats are diverse, and thus, as a group they are found across a wide range of environmental conditions such as temperature, salinity, dissolved oxygen concentrations, food availability, and redox conditions (reviewed in Murray 2006). It is therefore expected that foraminiferal lineages have specific physiological adaptations to their environments. Studying their cytoplasmic structure provides key clues to understanding these adaptations (Bernhard and Bowser 2008; Bernhard et al. 2006, 2010a, 2010b; Leutenegger and Hansen 1979). For instance, foraminiferal species inhabiting low oxygen habitats exhibit clusters of mitochondria just below the pores, openings in their calcite ($CaCO_3$) test that separate the outside environment from the cytoplasm within (Leutenegger and Hansen 1979). More recently, microscopic observations have been combined with novel techniques to provide useful insights on foraminiferal biology (Jauffrais et al. 2019; Khalifa et al. 2016) including metabolisms in oxygen-depleted environments (LeKieffre et al. 2017; Nomaki et al. 2016). Another metabolic adaptation to low oxygen environments is the symbiosis between foraminiferal host and endo- or ectosymbionts (reviewed in Bernhard et al. 2018). Recent studies on the metabolic capacity of

foraminifera revealed that substantial numbers of foraminiferal species perform denitrification under oxygen-depleted conditions (Glock et al. 2019; Risgaard-Petersen et al. 2006; Woehle et al. 2018).

Species of the genus *Chilostomella* Reuss 1849 are common in bathyal hypoxic sediments (Fontanier et al., 2005; Grimm et al. 2007; Nomaki et al. 2005b). Despite their common occurrences, little is known about their ecology. Benthic foraminifera show vertical microhabitat segregations in sediments depending on the food availability, oxygen concentration, nitrate concentration (all being typically lower in deeper sediments), and other environmental conditions (Jorissen et al. 1995; Koho et al. 2008; Zwaan et al., 1999). *Chilostomella ovoidea* (Fig. S1) is a deep-infaunal species most abundant in deep hypoxic sediments, but is also common at shallower depths in the sediments, unlike other typical deep infaunal foraminifera such as *Globobulimina* (Nomaki et al. 2005a, 2005b). In feeding experiments conducted by Nomaki et al. (2005a, 2006, 2011), many foraminiferal species preferably ingested algal organic matters, while *Chilostomella ovoidea* did not show any preferences across the range of food materials offered, that is, green algae, diatom, bacterium, and glucose. The carbon isotopic compositions ($\delta^{13}C$) of their sterols, reflecting both food sources and subsequent metabolism in *C. ovoidea*, were different from other species, suggesting *C. ovoidea* has unique food sources and/or metabolic pathways.

Interestingly, $\delta^{13}C$ values of their calcite test also differ from values of the ambient dissolved inorganic carbon (DIC) by 1‰, whereas other species have a calcite test having almost identical $\delta^{13}C$ values to those of the DIC. This may reflect a stronger "vital effect" than other species, such as a larger contribution of respired CO_2 to the DIC pool for calcification (McConnaughey et al. 1997).

All these observations indicate that *C. ovoidea* exhibits unique nutritional and metabolic adaptations that allow it to live across a wide depth range in the sediment from the oxic surface sediments to deep hypoxic sediments. Transmission electron microscope (TEM) observations of *C. ovoidea* indicated that the cytoplasm of this species typically possesses abundant electron-dense (either inherent or when stained with lead or osmium tetroxide) linear structures, usually < 1 μm thick and several tens of microns long. These highly abundant structures have not been reported from any other foraminiferal species, suggesting that they perform a function unique to this species or to the genus *Chilostomella*. Here, we present a detailed characterization of these structures, revealing their chitinous nature, three-dimensional distribution in a single test, and discuss their potential origin and possible roles in relation to the unique ecology of *C. ovoidea*.

MATERIALS AND METHODS

Foraminiferal sampling

Deep-sea sediments containing *Chilostomella ovoidea* were collected from central Sagami Bay, Japan, during cruise KS13-T2 of R/V *Shinsei-Maru* in October 2013 (34°58.0′N 139°23.9′E; water depth 1,480 m) and cruise KM16-01 of R/V *Kaimei* in April 2016 (35°01.3′N 139°22.1′E; water depth 1,430 m). Oxygen concentration of the bottom water in central Sagami Bay is between 55 and 59 μmol/L, and the average oxygen penetration depth in the sediment is 6.7 ± 2.5 mm (Glud et al. 2009).

During cruise KS13-T2, sediment samples were collected with a multiple corer and sliced immediately upon recovery on-board into 1-cm sections, to a depth of 6 cm. Sliced sections were preserved at 4 °C in separate plastic bags without additional seawater. In the laboratory, deep-sea bottom water was added to the sediment to remove fine particles by decantation, and foraminiferal specimens were collected immediately from the remaining sediments under a binocular stereomicroscope. Thirteen specimens of *C. ovoidea* were collected from the 4–5 cm depth section and were fixed overnight in 2.5% glutaraldehyde in filtered seawater and stored at 4 °C (Nomaki et al. 2015b).

During cruise KM16-01, sediment samples were collected with a push corer attached to the remotely operated vehicle *KM-ROV* and were immediately sliced on-board into 0.5- or 1-cm sections to a depth of 6 cm. The sediment samples were fixed in 10% glutaraldehyde to a final concentration of 4.0% glutaraldehyde (Nomaki et al. 2018). In the laboratory, specimens with an aggregation of sediment particles around their apertures and/or with tests mostly filled with cytoplasm were isolated from the > 125-μm size fraction using a binocular stereomicroscope. Three isolated specimens from the 1–2 cm depth sections were preserved in 2.5% glutaraldehyde in filtered seawater and stored at 4 °C prior to further processing.

Preparation of epoxy embedded foraminiferal specimens

Sample fixation, uranium staining, and subsequent resin embedding followed previously published protocols for TEM sample preparation (Nomaki et al. 2014, 2015b; Tsuchiya et al. 2015). In brief, fixed foraminiferal specimens (13 specimens from KS13-T2, 2 specimens from KM16-01) were embedded in 1% aqueous agarose and then cut into approximately 1 mm^3 cubes. The specimens were decalcified with 0.2% EGTA in 0.81 mol/L aqueous sucrose solution (pH 7.0) for several days, rinsed with 0.22-μm- filtrated artificial seawater (FASW) (REI-SEA Marine II, Iwaki co., Ltd., Tokyo, Japan), and then postfixed with 2% osmium tetroxide in FASW for 2 h at 4 °C. Specimens were rinsed with an 8% aqueous sucrose solution and stained *en bloc* with 1% aqueous uranyl acetate for 2 h at room temperature. Stained specimens were rinsed with distilled water, dehydrated in a graded ethanol series, and embedded in epoxy resin (Quetol 651; Nisshin EM, Tokyo, Japan).

Cellular ultrastructure observations

A number of embedded specimens were sectioned into several semi-thin sections (500 nm thick) using an

ultramicrotome (Ultracut S, Leica, Wetzlar, Germany). They were observed with an optical microscope (BX51, Olympus, Tokyo, Japan) to assess the condition of the cytoplasm and distribution of linear and curved structures. Four specimens from KS13-T2 and two specimens from KM16-01 were further sectioned into ultra-thin sections (60 nm thick). The sections were stained with 2% aqueous uranyl acetate and lead staining solution (0.3% lead nitrate and 0.3% lead acetate, Sigma-Aldrich Japan, Tokyo, Japan) and were observed by TEM (Tecnai 20, FEI, Portland, Oregon, USA) operated at 120 kV.

Serial sectioning and 3D reconstruction

A single *C. ovoidea* individual from KM16-01 was cut into 432 serial, semi-thin sections, each 500 nm thick, using the ultramicrotome. The serial semi-thin sections of the complete foraminifera were sequentially imaged with a digital camera mounted on an optical microscope (BX51, Olympus). Obtained images were rotated to the same overall orientation and batch processed for contrast adjustments and size reduction in Adobe Photoshop CC. The images were then imported into Amira 6.2 (Thermo Fisher Scientific, Waltham, MA, USA) and aligned into a single stack. Structures of interest, particularly the linear structures characteristic of *C. ovoidea*, were highlighted manually throughout all 432 slices. The highlighted linear structures were grouped according to which chamber they occurred in. In order to generate the final tomographic model, the resulting groups were subjected to a series of postprocessing in Amira 6.2, as follows. Firstly, the segmentation data were rendered into 3D surfaces (i.e. the 3D model) using the "SurfaceGen" function with the default "constrained smoothing" settings and checked for completeness. Secondly, the model was smoothed twice using the "SmoothSurface" function with strength ("lambda") set to 0.8. Finally, each chamber group of linear structures was extracted separately as a separate 3D surface using the "ExtractSurface" function in order to change display settings such as coloration for each group. Once display settings were completed, all groups were set to display simultaneously, resulting in the final model. For further details, we refer to previously published methods which we followed (Ruthensteiner 2008; Sigwart et al. 2014).

Histochemical staining

Several specimens were fixed with 4% paraformaldehyde in FASW for at least 24 h at 4 °C. The fixed specimens were washed with FASW, embedded in 1.0% agarose in Milli-Q water, and decalcified with 0.2% EGTA as described above. The agarose gel blocks containing the specimens were then washed with FASW, dehydrated using a graded ethanol series, and embedded in Technovit 8100 resin (Heraeus Kulzer Ltd., Hanau, Germany) at 4 °C. Semi-thin sections (2 μm thick) were prepared using a glass knife mounted on the ultramicrotome and collected on glass slides.

Two different dyes were used to test the composition of the observed structures: Calcofluor white and Congo red. While both Calcofluor white and Congo red stain cellulose (Trivedi et al., 2016), only Calcofluor white stains chitin (Harrington and Hageage 2003). For Calcofluor white, the sections were incubated for 2 min at room temperature, with the Calcofluor white solution prepared from a Fungi-Fluor® kit (Polysciences, Inc., Warrington, PA, USA) according to the manufacturer's protocol. The fluorescence signals were observed using a BX51 fluorescence microscope (Olympus), equipped with a UV-1A filter (an excitation wavelength of 345–365 nm and emission wavelength > 400 nm). For Congo red, the sections were stained for 30 min at room temperature, with Congo red solution containing with 0.2% Congo red, 1.5% NaCl, 0.1% NaOH, and 80% ethanol. After washing with Milli-Q water, they were mounted on a glass slide using a mounting medium (Merck), cover-slipped, and observed under an optical microscope (BX51, Olympus).

RESULTS

Observations with optical microscope and TEM

All observed specimens possessed abundant linear or arc-like structures in almost all chambers (Fig. 1). In some cases, the linear structures in *Chilostomella ovoidea* were located along a vacuole membrane (Fig. 1B) or were found to form a part of the vacuole membrane (Fig. 1F). The linear structures were sometimes oriented in particular directions within a chamber (Fig. 1G, H, 2A), while in some other cases they were curved or spiral in shape (Fig. 2C). The linear structures appeared to separate the cytoplasm containing mitochondria and peroxisome (Fig. 1D, H, 2B), while no cytoplasm was observed inside the spiral shapes (Fig. 2C). The thickness of the structures varied from approximately 200 nm to 1 μm, and the length was generally several 10s of μm (Fig. 2A, B). Detailed observations of the structures revealed that some consisted of several layers of fibrils with a probable width of some 10s of nm (Fig. 2D).

Histochemical staining

The observed linear and spiral structures were stained with Calcofluor white, which stains both chitin and cellulose (Fig. 3A–D). Additional staining with Congo red, which stains cellulose but not chitin, did not show obvious staining of those structures in *C. ovoidea* (Fig. 3E, F). A positive staining test using known cellulose structures confirmed Congo red staining on cellulose with the same procedure (not shown).

Three-dimensional reconstruction

Three-dimensional reconstruction of the linear, curved, and spiral structures throughout the entire specimen with nine chambers showed that the structures are present in the final seven chambers but absent in the first two

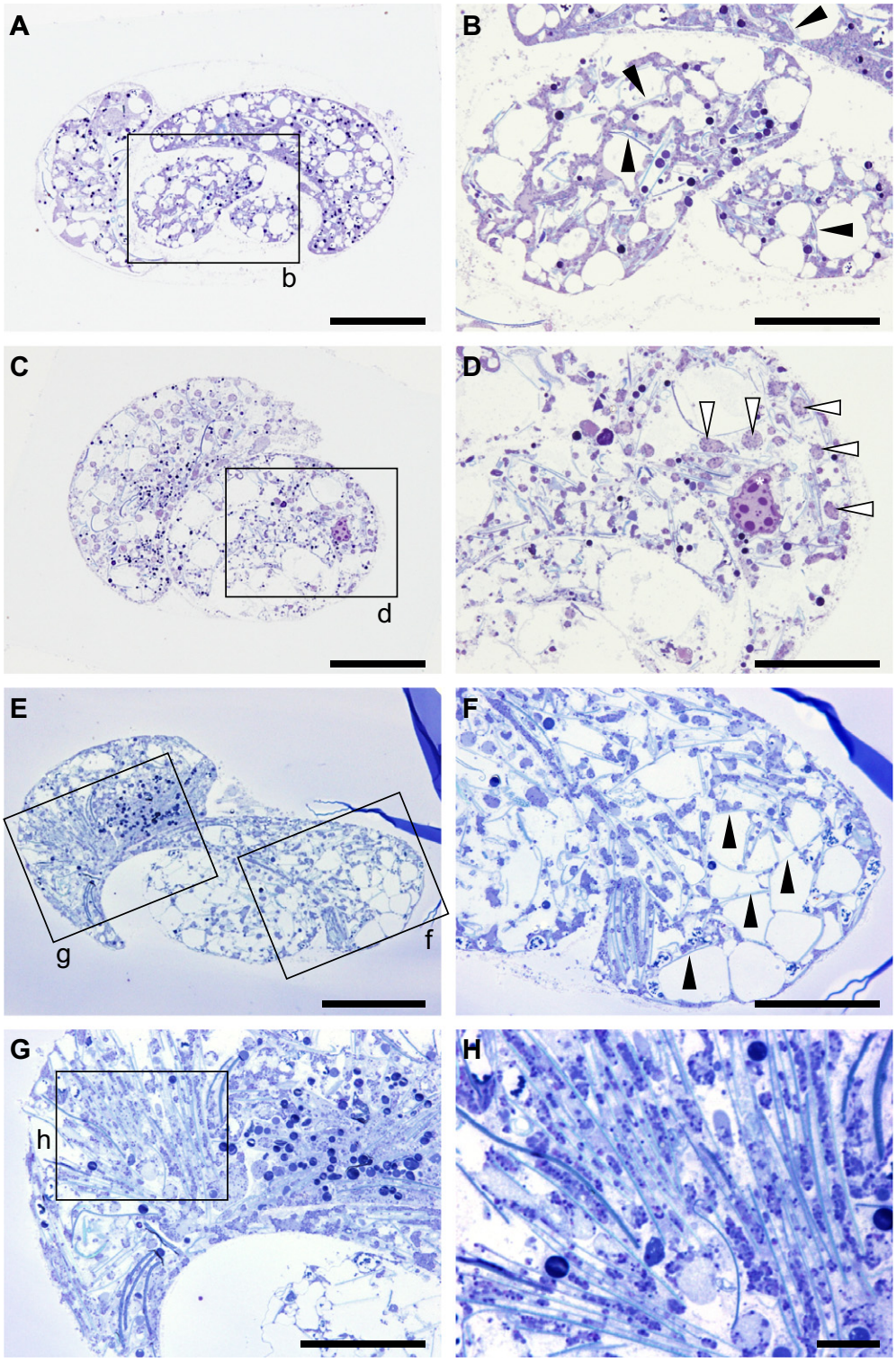

Figure 1 Optical micrographs of *Chilostomellaovoidea*. (**A**) Longitudinal section through a specimen, (**B**) A close-up view of the rectangle (b) in the image A, showing chitinous plates forming a part of the vacuole wall (black arrows), (**C**) latitudinal section through a specimen, (**D**) a close-up view of the rectangle (d) in the image C, showing nucleus (*) and cytoplasms (white arrows), (**E**) longitudinal section through a specimen, (**F**) a close-up view of the rectangle (f) in the image E, showing chitinous plates forming a part of the vacuole wall (black arrows), (**G**) a close-up view of the rectangle (g) in the image E, and (**H**) a close-up view of the rectangle (h) in the image G, both showing particular orientation of chitinous plates in between cytoplasm. Parts A, C, and E were taken from different specimens. Scales bars: A, C, E = 100 μm; B, D, F, G = 50 μm; H = 10 μm.

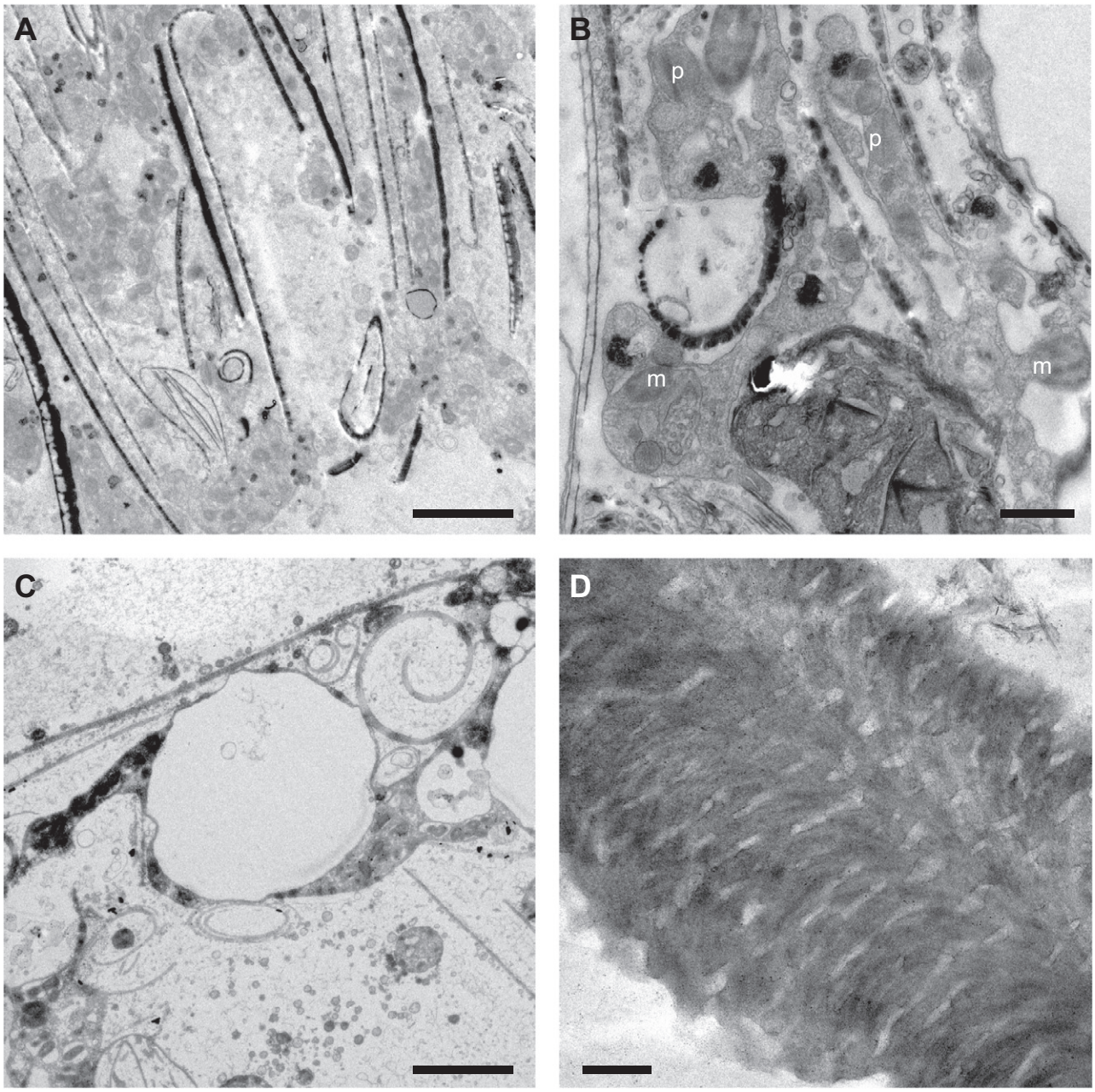

Figure 2 2Ultrastructural observations of *Chilostomellaovoidea*. (**A**) TEM image of chitinous structures partitioning the cytoplasm, showing most chitinous structures aligned to the same orientation (**B**) A close-up view of chitinous structures and the cytoplasm, m: mitochondria, p: peroxisome, (**C**) chitinous structures showing rolled, spiral form, (**D**) a close-up view of a section through the chitinous structure showing the fibrils comprising it. Scales bars: A, C = 5 μm; B = 1 μm; D = 200 nm.

(Fig. 4). It should be noted that the thickness of the plate structures shown on the images does not represent the true thickness, due to surface smoothing during processing. Also, the stepped impression of the surfaces along the X-Y plane is artifacts resulting from the boundary between two sections.

Chilostomella periodically and sequentially add chambers when growing, by surrounding old chambers (bottom side of Fig. 4B, I) with newer chambers. In the last two chambers, plate-like structures are dominant. These are generally oriented parallel to the calcite test. At the edge of the chamber, some plates were rolled up and exhibited a cigar-like, rolled morphology. In the older chambers, the ratio of cigar-like structures increased relative to plate-like structures (Fig. 4). In the 3rd to 6th chambers, most of the structures were cigar-like.

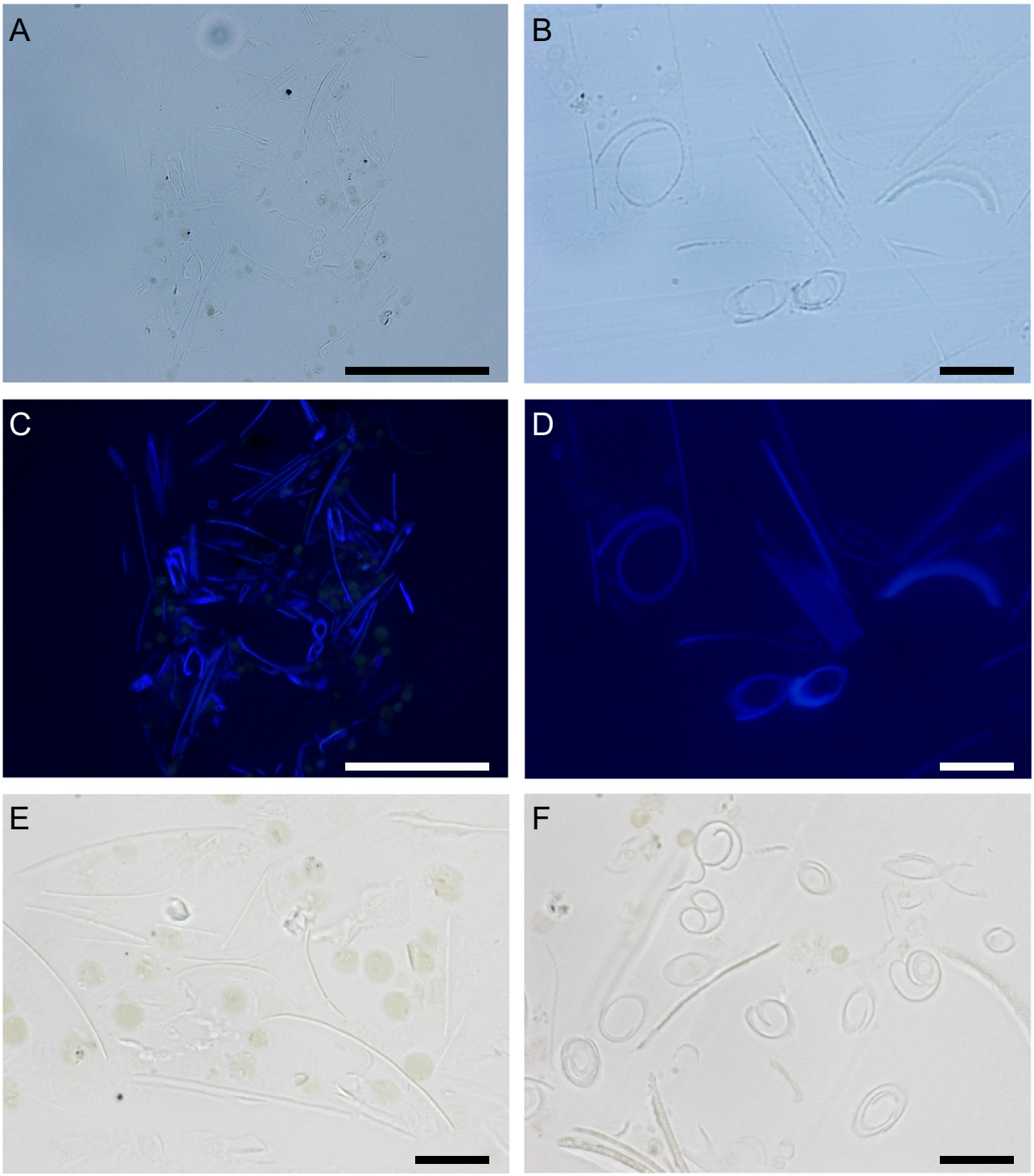

Figure 3 Histochemical staining images using Calcofluor white (**A–D**) and Congo red (**E and F**). (A and B) optical microscopic views of the chitinous structures. (C and D) Fluorescent microscopic views with a UV-1A filter (an excitation wavelength of 345–365 nm and emission wavelength > 400 nm) of the same view as A and B, respectively. (E and F) Optical microscopic view of the chitinous structure after Congo red staining. No staining on the chitinous structures could be detected. Scale bars: A, C = 50 μm; B, D, E, F = 10 μm.

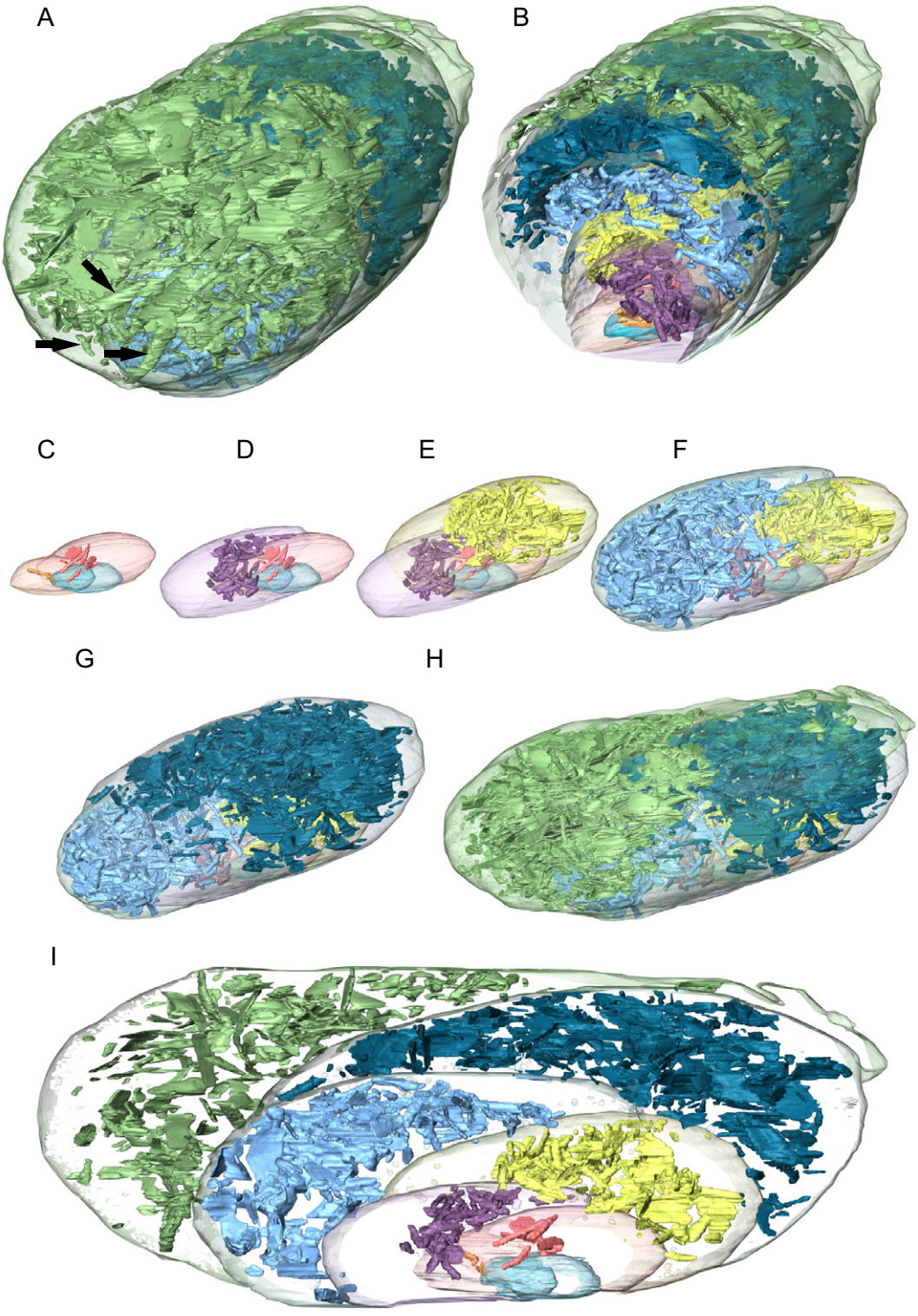

Figure 4 Renders of the 3D reconstruction showing the distribution of chitinous structures in an entire specimen of *Chilostomellaovoidea*. (**A**) View of the entire specimen showing the newest chamber in the foreground. Black arrows indicate cigar-like structures. (**B**) A cross section through the same reconstructed specimen showing the distribution of chitinous structures in different chambers (marked with different colors). (**C**) 1st to 4th chambers, (**D**) 1st to 5th chambers, (**E**) 1st to 6th chambers, mostly cigar-like structures, (**F**) 1st to 7th chambers, showing some plate-like structures in the 7th chamber, (**G**) 1st to 8th chambers, (**H**) 1st to 9th chambers, with those in 8th and 9th chambers mainly consisting of plate-like structures. (**I**) Longitudinal section of the 3D reconstruction showing the 1st chamber through to the 9th chamber.

DISCUSSION

Distributions of chitinous structures in the cytoplasm

Based on the histochemical staining results, the linear and arc-like structures are chitinous in nature. The minute mass of chitin in *Chilostomella ovoidea* makes it impractical to apply further characterization techniques such as X-ray diffraction analyses, ^{13}C CP/MAS nuclear magnetic resonance (NMR) (Isobe et al. 2020), or electron diffraction analyses (Rinaudo 2006). It remains unclear, therefore, whether the chitin in *C. ovoidea* is α-chitin, the abundant form used by organisms that occurs in biological structures such as fungal and yeast cell walls as well as arthropod exoskeletons (Rinaudo 2006), or β-chitin, the less common form known to occur in siboglinid worm tubes (Graill et al. 1992), in the loricas of chrysophytes (Herth et al. 1977), and the ciliate *Eufolliculina uhligi* (Herth et al. 1986), among others. The ultrastructure of a section through the chitinous plate (Fig. 2D) in *C. ovoidea* resembles the chitin observed in the soft membrane of the American lobster *Homarus americanus* (Wu et al. 2019), but is dissimilar to the structures seen in *E. uhligi* (Herth et al. 1986).

The chitinous structures in *C. ovoidea* exhibited mostly plate-like morphologies in the newer chambers and curved, rolled, cigar-like shapes in the older chambers (and the periphery of the newer chambers). This indicates that the cigar-like structures may be expended forms of the plate-like structures that became rolled after use. From the TEM images, the cigar-like structures were not surrounded by cytoplasm (Fig. 1E), suggesting once the structure has lost the cytoplasmic support, they become rolled up. In the older chambers where the cytoplasm was sparse, only cigar-like structures were observed (Fig. 4C, D).

Origin of chitinous structures and characteristic isotopic compositions of *C. ovoidea*

There is no direct evidence to determine whether the chitinous structures are synthesized by *C. ovoidea* itself or incorporated from outside sources. The chitinous plates are of sizes that can fit into the aperture of *C. ovoidea*, the primary opening of the newest chamber in the calcite test connecting the interior to surrounding environments. It is possible that *C. ovoidea* incorporate these chitinous plates through feeding on particular organisms, such as algae with chitinous cell walls or arthropods such as benthic copepods with chitinous exoskeletons (Jeuniaux et al. 1986). A spiral structure somewhat similar to those observed in *C. ovoidea* was reported from *Quinqueloculina seminula* and was speculated to be an algal cell wall (Heeger 1990). A food vacuole containing copepod muscle tissue was observed in *Miliolinella subrotunda* (Linke et al. 1995). However, vacuoles of *C. ovoidea* are typically empty (Fig. 1A–F) and show no apparent evidence for either selective feeding on algae or arthropods or deposit feeding on sediment that potentially include such organisms. Furthermore, trophic position determinations based on the amino acid nitrogen isotopic composition (Chikaraishi et al. 2009) of *C. ovoidea* were 2.4 ± 0.1, suggesting that small benthic arthropods with chitinous exoskeletons (supposed to have trophic positions higher than 2) are not major food sources of *C. ovoidea* (Nomaki et al. 2015a). This indicates that the chitinous structures seen in *C. ovoidea* are unlikely to be arthropod remnants.

Some foraminiferal species have been reported to possess chitinous shells or agglutinated tests with sand grains attached to a chitinoid wall (Thalmann and Bermudez 1954), although no clear evidences have been published to confirm their chitinous nature. Some earlier studies used the terms "tectin" or "pseudochitin" without any specific chemical definition, but Hedley (1963) criticized the use of such terms and concluded that the cement of some agglutinated foraminifera consists of organic materials, but not chitin. If *C. ovoidea* synthesizes the chitinous plates by itself, the energetic cost can be expected to be substantial, considering the large quantity of chitinous plates in a single specimen (Fig. 4). As mentioned previously, the carbon isotopic compositions of some sterols (C numbers of 28 and 29) in *C. ovoidea* were 2–4‰ heavier than those of other foraminiferal species (H. Nomaki unpublished data). An isotope labeling study showed that *Globobulimina affinis*, another deep-infaunal foraminifera species, synthesize these sterols within several days of incubation, suggesting that foraminifera can synthesize or modify these C_{28} and C_{29} sterols (Nomaki et al. 2009). We speculate that because the synthetic cost of the chitinous plates is substantial, the balance of C metabolism in *C. ovoidea* is likely to be different from other foraminiferal species. For instance, ^{12}C may be preferentially used for chitinous plate synthesis and other organic compounds consequently become enriched in ^{13}C. Differences in $\delta^{13}C$ values between chitinous exoskeletons and soft tissue have been reported for some crustaceans, including by 1.5‰ in the green crab *Carcinus maenas* (Curtis et al. 2017), supporting this speculation. However, we cannot evaluate these factors quantitatively because the information on the synthetic pathway of chitin in foraminifera, and its frequency and turnover rates are not available.

Potential functions of the structure

The large numbers of chitinous structures observed in *Chilostomella ovoidea* suggest that they have some functions specific to this species or this genus, since such structures were not observed in other co-occurring species. Here, we suggest two possible explanations for their occurrence.

Partitioning the cytoplasm and enlarging the surface-to-volume ratio

The cytoplasm of *C. ovoidea* was finely partitioned by the chitinous structures (Fig. 1). Foraminifera take up some ions and chemicals from surrounding seawater for their nutrition and metabolism (de Nooijer et al. 2008; Kuile et al. 1989; Lee et al. 1966), and thus, it is beneficial for the cytoplasm to have a higher surface-to-volume ratio to

facilitate such exchanges. Expansion of reticulopodia, part of the cytoplasm, is common in many foraminifera. Although reticulopodia also have many other functions (Travis and Bowser 1991), one of the functions of its expansion is considered to increase the surface-to-volume ratio. Possessing the abundant vacuoles in the cytoplasm (e.g. allogromiids, reported in Bernhard et al. 2006) may also function to increase the surface-to-volume ratio between cytoplasm and intracellular seawater. *Chilostomella ovoidea* does not have noticeably branched reticulopodia (Fig. S1D, E), while the co-occurring deep-sea foraminifera *Bulimina aculeata* and *Globobulimina affinis* deploy branched reticulopodia. It is possible that *C. ovoidea* uses these chitinous plates to separate the cytoplasm into compartments (Fig. 1H, 2B) as an alternative adaptive strategy to increase the surface-to-volume ratio of cytoplasm inside the calcitic test. The chitinous plates may also help to prevent the merging of segmentalized cytoplasm. The toughness of chitin makes it a good material for exoskeletons or cell walls of many aquatic organisms, from unicellular organisms to invertebrates. Chitinous plates in *C. ovoidea* may function as a cytoskeleton to structure the cytoplasm with a high surface-to-volume ratio.

Reactive site for metabolic functions

In addition to increasing the surface-to-volume ratio of the cytoplasm, the large surface area of chitinous plates may also play significant roles in metabolic functions of *C. ovoidea*. As observed in Fig. 2D, the chitinous plates exhibit a chiral-nematic ordering typical of chitin nanofibers, similar to the chitinous soft membrane in the American lobster *Homarus americanus* (Wu et al. 2019). Such a nanofibrous structure with a width between 10 and 30 nm generates a large specific surface area of ca. 100 m^2/g at a conservative estimation. This large surface area enhances the chemical properties of functional groups on chitin, specifically the amino groups at C2 position of glucosamine units.

Chitin is a linear polysaccharide made of *N*-acetyl glucosamine residues, where the amino groups at the C2 position are mostly acetylated. However, we know that about 10% of the total amino groups at the C2 position in the native chitin is in the deacetylated form (Hackett and Chen 1978; Rinaudo 2006) and therefore available as a reactive functional group. Two possible roles of the free amino group of chitin in *C. ovoidea* are: as (1) selective adsorption sites and (2) catalytic sites.

The amino groups in chitin have a selective adsorption capacity for metal ions, such as copper ions (Rhazi et al. 2002), through chelate formation between copper ions and amino groups (Rhazi et al. 2001). The adsorption capacity is further enhanced when pH is higher than 6 (Juang and Shao 2002), a condition commonly observed in the cytoplasm of various foraminiferal species (de Nooijer et al. 2008). Copper ions are indispensable for many proteins, such as cytochrome *c* oxidase, and also for the catalytic domain of nitrite reductase in *Globobulimina* (Woehle et al. 2018). The large surface area of the chitinous plates may facilitate the adsorption of copper and other metal ions from incorporated seawater for protein synthesis.

Another potential function of the chitinous plates is to serve as a site for the catalysis of some chemical reactions on the plate surface. The free amino groups at the C2 position in chitin are known to function as a base catalyst (Hirayama et al. 2020; Tsutsumi et al. 2014). Many reactions have been reported to be facilitated by the free amino groups at the C2 position: a variety of C–C bond forming reactions including aldol reactions, Knoevenagel condensation, nitroaldol reaction, Michael reaction (Kühbeck et al. 2012), and the synthesis of α-amino nitriles and imines (Dekamin et al. 2013). Among these, Knoevenagel condensation is known to play a pivotal role in the total synthesis of organic compounds (Heravi et al. 2020), including sterols (List 2010; Woodward et al. 1952). Since chitinous plates in *C. ovoidea* are sometimes located along the vacuole membrane or even form a part of the vacuole membrane (Fig. 1B, F), they may facilitate particular reactions using compound(s) in vacuoles. Without detailed understanding of the ultrastructure of these chitinous plates and the contents of vacuoles in *C. ovoidea*, we cannot confirm if these structures actually play such catalytic roles. However, if chitinous plate does play a catalytic role, it can explain both the metabolic advantages of chitinous plates and the characteristic $\delta^{13}C$ values of organic compounds including sterols in *C. ovoidea*.

Comparative studies of the abundance and distribution of *C. ovoidea* in different habitats and its different growth stages will also help shed light on the true function of these chitinous structures. If these chitinous plates function to enlarge the surface-to-volume ratio, there may be a relationship between numbers of chitinous plates and some environmental factors. For instance, a higher surface-to-volume ratio may be advantageous in an environment with lower dissolved oxygen concentrations. Detailed observation of the chitinous plates in juvenile specimens may also provide some important insights, such as whether the rolled, cigar-like structures in older chambers (i.e. grown during the juvenile stage) were indeed originally plate-like. Maintaining this deep-sea species, which probably has a lifespan exceeding two years (Ohga and Kitazato 1997), is still challenging in a laboratory, hampering experimental studies to investigate the function of its characteristic chitinous structures. Future genomic study of this species may resolve whether it is capable of synthesizing chitin, the characteristic carbon isotopic composition of organic compounds such as sterols, and more generally its metabolic adaptations to hypoxic deep-infaunal sediments.

ACKNOWLEDGMENTS

We are grateful to Drs. Tomo Kitahashi and Koji Seike, as well as captain and crew of both R/V *Shinsei-maru* during cruise KS13-T2 and R/V *Kaimei* during cruise KM16-01 for their help in obtaining the surface sediment samples. We thank two anonymous reviewers and the editor, who

provided helpful comments on an earlier version of this manuscript. This work was supported by a Grant-in-Aid for Scientific Research from the Ministry of Education, Culture, Sports, Science and Technology, Japan (Scientific Research C 17K05697 to HN).

LITERATURE CITED

Bernhard, J. M. & Bowser, S. S. 2008. Peroxisome proliferation in foraminifera inhabiting the chemocline: an adaptation to reactive oxygen species exposure? *J. Eukaryot. Microbiol.*, 55:135–144.

Bernhard, J. M., Goldstein, S. T. & Bowser, S. S. 2010a. An ectobiont-bearing foraminiferan, *Bolivina pacifica*, that inhabits microxic pore waters: cell-biological and paleoceanographic insights. *Environ. Microbiol.*, 12:2107–2119.

Bernhard, J. M., Habura, A. & Bowser, S. S. 2006. An endobiont-bearing allogromiid from the Santa Barbara Basin: implications for the early diversification of foraminifera. *J. Geophys. Res.*, 111:G03002.

Bernhard, J. M., Martin, J. B. & Rathburn, A. E. 2010b. Combined carbonate carbon isotopic and cellular ultrastructural studies of individual benthic foraminifera: 2. Toward an understanding of apparent disequilibrium in hydrocarbon seeps. *Paleoceanography*, 25:PA4206.

Bernhard, J. M., Tsuchiya, M. & Nomaki, H. 2018. Ultrastructural observations on bacterial associates of benthic foraminifera: food, mutualistic symbionts, or parasites? *Mar. Micropaleontol.*, 138:33–45.

Chikaraishi, Y., Ogawa, N. O., Kashiyama, Y., Takano, Y., Suga, H., Tomitani, A., Miyashita, H., Kitazato, H. & Ohkouchi, N. 2009. Determination of aquatic food-web structure based on compound-specific nitrogen isotopic composition of amino acids. *Limnol. Oceanogr. Meth.*, 7:740–750.

Curtis, A. N., Bugge, D. M., Buckman, K. L., Feng, X., Faiia, A. & Chen, C. Y. 2017. Influence of sample preparation on estuarine macrofauna stable isotope signatures in the context of contaminant bioaccumulation studies. *J. Exp. Mar. Biol. Ecol.*, 493:1–6.

de Nooijer, L. J., Toyofuku, T., Oguri, K., Nomaki, H. & Kitazato, H. 2008. Intracellular pH-distribution in foraminifera determined by the fluorescent probe HPTS. *Limnol. Oceanogr-Meth.*, 6:610–628.

Dekamin, M. G., Azimoshan, M. & Ramezani, L. 2013. Chitosan: a highly efficient renewable and recoverable bio-polymer catalyst for the expeditious synthesis of α-amino nitriles and imines under mild conditions. *Green Chem.*, 15:811–820.

Fontanier, C., Jorissen, F. J., Chaillou, G., Anschutz, P., Gremare, A. & Griveaud, C. 2005. Live foraminiferal faunas from a 2800 m deep lower canyon station from the Bay of Biscay: faunal response to focusing of refractory organic matter. *Deep-Sea Res. Pt I*, 52:1189–1227.

Glock, N., Roy, A., Romero, D., Wein, T., Weissenbach, J., Revsbech, N. P., Høgslund, S., Clemens, D., Sommer, S. & Dagan, T. 2019. Metabolic preference of nitrate over oxygen as an electron acceptor in foraminifera from the Peruvian oxygen minimum zone. *Proc. Natl. Acad. Sci. USA*, 116:2860–2865.

Glud, R. N., Stahl, H., Berg, P., Wenzhoefer, F., Oguri, K. & Kitazato, H. 2009. In situ microscale variation in distribution and consumption of O_2: a case study from a deep ocean margin sediment (Sagami Bay, Japan). *Limnol. Oceanogr.*, 54:1–12.

Graill, F., Persson, J., Sugiyama, P., Vuong, R. & Chanzy, H. 1992. The chitin system in the tubes of deep sea hydrothermal vent worms. *J. Struct. Biol.*, 109:116–128.

Grimm, G. W., Stögerer, K., Ertan, K. T., Kitazato, H., Kučera, M., Hemleben, V. & Hemleben, C. 2007. Diversity of rDNA in *Chilostomella*: molecular differentiation patterns and putative hermit types. *Mar. Micropaleontol.*, 62:75–90.

Hackett, C. J. & Chen, K. C. 1978. Quantitative isolation of native chitin from resistant structures of *Sordaria* and *Ascaris* species. *Anal. Biochem.*, 89:487–500.

Harrington, B. J. & Hageage, G. J. 2003. Calcofluor white: a review of its uses and applications in clinical mycology and parasitology. *Lab. Med.*, 34:361–367.

Hedley, R. H. 1963. Cement and iron in the arenaceous foraminifera. *Micropaleontology*, 9:433–441.

Heeger, T. 1990. Elektronenmikroskopische Untersuchungen zur Ernährungsbiologie benthischer Foraminiferen. *Ber. Sonderforsch.*, 313:1–139.

Heravi, M. M., Janati, F. & Zadsirjan, V. 2020. Applications of Knoevenagel condensation reaction in the total synthesis of natural products. *Monatshefte Chem. Chem. Mon.*, 151:439–482.

Herth, W., Kuppel, A. & Schnepf, E. 1977. Chitinous fibrils in the lorica of the flagellate Chrysophyte *Poteriochromonas stipitate* (syn. *Ochromonas malhamensis*). *J. Cell Biol.*, 73:311–321.

Herth, W., Mulisch, M. & Zugenmaier, P. 1986. Comparison of chitin fibril structure and assembly in three unicellular organisms. *In*: Muzzarelli, R., Jeuniaux, C. & Gooday, G. W. (ed.), Chitin in Nature and Technology. Plenum Publishing Corporation, New York, NY. p. 107–120.

Hirayama, Y., Kanomata, K., Hatakeyama, M. & Kitaoka, T. 2020. Chitosan nanofiber-catalyzed highly selective Knoevenagel condensation in aqueous methanol. *RSC Adv.*, 10:26771.

Isobe, N., Tsudome, M., Kusumi, R., Wada, M., Uematsu, K., Okada, S. & Deguchi, S. 2020. Moldable crystalline α-chitin hydrogel with toughness and transparency toward ocular applications. *ACS Appl. Polym. Mater.*, 2:1656–1663.

Jauffrais, T., LeKieffre, C., Schweizer, M., Geslin, E., Metzger, E., Bernhard, J. M., Jesus, B., Filipsson, H. L., Maire, O. & Meibom, A. 2019. Kleptoplastidic benthic foraminifera from aphotic habitats: insights into assimilation of inorganic C, N and S studied with sub-cellular resolution. *Environ. Microbiol.*, 21:125–141.

Jeuniaux, C., Bussers, J. C., Voss-Foucart, M. F. & Poulicek, M. 1986. Chitin production by animals and natural communities in marine environment. *In*: Muzzarelli, R., Jeuniaux, C. & Gooday, G. W. (ed.), Chitin in Nature and Technology. Plenum Publishing Corporation, New York, NY. p. 515–522.

Jorissen, F. J., de Stigter, H. C. & Widmark, J. G. V. 1995. A conceptual model explaining benthic foraminiferal microhabitats. *Mar. Maicropal.*, 26:3–15.

Juang, R. S. & Shao, H. J. 2002. Effect of pH on competitive adsorption of Cu(II), Ni(II), and Zn(II) from water onto chitosan beads. *Adsorption*, 8:71–78.

Khalifa, G. M., Kirchenbuechler, D., Koifman, N., Kleinerman, O., Talmon, Y., Elbaum, M., Addadi, L., Weiner, S. & Erez, J. 2016. Biomineralization pathways in a foraminifer revealed using a novel correlative cryo-fluorescence-SEM-EDS technique. *J. Struct. Biol.*, 196:155–163.

Koho, K. A., García, R., de Stigter, H. C., Epping, E., Koning, E., Kouwenhovern, T. J. & van der Zwaan, G. J. 2008. Sedimentary labile organic carbon and pore water redox control on species distribution of benthic foraminifera: a case study from Lisbon-Setúbal Canyon (southern Portugal). *Progr. Oceanogr.*, 79:55–82.

Kühbeck, D., Saidulu, G., Reddy, K. R. & Díaz, D. D. 2012. Critical assessment of the efficiency of chitosan biohydrogel beads as

recyclable and heterogeneous organocatalyst for C−C bond formation. *Green Chem.*, 14:378–392.

Kuile, B., Erez, J. & Padan, E. 1989. Mechanisms for the uptake of inorganic carbon by two species of symbiont-bearing foraminifera. *Mar. Biol.*, 103:241–251.

Lee, J. J., McEnery, M., Pierce, S., Freudenthal, H. D. & Muller, W. A. 1966. Tracer experiments in feeding littoral foraminifera. *J. Protozool.*, 13:659–670.

LeKieffre, C., Spangenberg, J. E., Mabilleau, G., Escrig, S., Meibom, A. & Geslin, E. 2017. Surviving anoxia in marine sediments: the metabolic response of ubiquitous benthic foraminifera (*Ammonia tepida*). *PLoS One*, 12(5):e0177604.

Leutenegger, S. & Hansen, H. J. 1979. Ultrastructural and Radiotracer studies of pore function in foraminifera. *Mar. Biol.*, 54:1–16.

Linke, P., Altenbach, A. V., Graf, G. & Heeger, T. 1995. Responses of deep-sea benthic foraminifera to a simulated sedimentation event. *J. Foraminifer. Res.*, 25:75–82.

List, B. 2010. Emil Knoevenagel and the roots of aminocatalysis. *Angew. Chem. Int. Ed.*, 49:1730–1734.

McConnaughey, T. A., Burdett, J., Whelan, J. F. & Paull, C. K. 1997. Carbon isotopes in biological carbonates: respiration and photosynthesis. *Geochim. Cosmochim. Acta*, 61:611–622.

Murray, J. H. 2006. Ecology and applications of benthic foraminifera. Cambridge University Press, Cambridge. p. 426.

Nomaki, H., Bernhard, J. M., Ishida, A., Tsuchiya, M., Uematsu, K., Tame, A., Kitahashi, T., Takahata, N., Sano, Y. & Toyofuku, T. 2016. Intracellular isotope localization in *Ammonia* sp. (Foraminifera) of oxygen-depleted environments: results of nitrate and sulfate labeling experiments. *Front. Microbiol.*, 7:163.

Nomaki, H., Chikaraishi, Y., Tsuchiya, M., Toyofuku, T., Ohkouchi, N., Uematsu, K., Tame, A. & Kitazato, H. 2014. Nitrate uptake by foraminifera and use in conjunction with endobionts under anoxic conditions. *Limnol. Oceanogr.*, 59:1879–1888.

Nomaki, H., Chikaraishi, Y., Tsuchiya, M., Toyofuku, T., Suga, H., Sasaki, Y., Uematsu, K., Tame, A. & Ohkouchi, N. 2015a. Variation in the nitrogen isotopic composition of amino acids in benthic foraminifera: implications for their adaptation to oxygen-depleted environments. *Limnol. Oceanogr.*, 60:1906–1916.

Nomaki, H., Heinz, P., Hemleben, C. & Kitazato, H. 2005a. Behaviors and responses of deep-sea benthic foraminifera to freshly supplied organic matter: laboratory feeding experiments in microcosm environments. *J. Foramin. Res.*, 35:103–113. https://doi.org/10.2113/35.2.103

Nomaki, H., Heinz, P., Nakatsuka, T., Shimanaga, M. & Kitazato, H. 2005b. Species-specific ingestion of organic carbon by deep-sea benthic foraminifera and meiobenthos: in situ tracer experiments. *Limnol. Oceanogr.*, 50:134–146.

Nomaki, H., Heinz, P., Nakatsuka, T., Shimanaga, M., Ohkouchi, N., Ogawa, N. O., Kogure, K., Ikemoto, E. & Kitazato, H. 2006. Different ingestion patterns of ^{13}C-labeled bacteria and algae by deep-sea benthic foraminifera. *Mar. Ecol. Progr. Ser.*, 310:95–108.

Nomaki, H., LeKieffre, C., Meibom, A., Escrig, S., Yagyu, S., Richardson, E. A., Matsuzaki, T., Murayama, M., Geslin, E. & Bernhard, J. M. 2018. Innovative TEM-coupled approaches to study foraminiferal cells. *Mar. Micropaleontol.*, 138:90–104.

Nomaki, H., Ogawa, N. O., Takano, Y., Suga, H., Ohkouchi, N. & Kitazato, H. 2011. Differing utilization of glucose and algal particulate organic matter by deep-sea benthic organisms of Sagami Bay, Japan. *Mar. Ecol. Progr. Ser.*, 431:11–24.

Nomaki, H., Ohkouchi, N., Heinz, P., Suga, H., Chikaraishi, Y., Ogawa, N. O., Matsumoto, K. & Kitazato, H. 2009. Degradation of algal lipids by deep-sea benthic foraminifera: an *in situ* tracer experiment. *Deep-Sea Res. Pt I*, 56:1488–1503.

Nomaki, H., Toyofuku, T., Tsuchiya, M., Matsuzaki, T., Uematsu, K. & Tame, A. 2015b. Three-dimensional observation of foraminiferal cytoplasmic morphology and internal structures using uranium–osmium staining and micro-X-ray computed tomography. *Mar. Micropaleontol.*, 121:32–40.

Ohga, T. & Kitazato, H. 1997. Seasonal changes in bathyal foraminiferal populations in response to the flux of organic matter (Sagami Bay, Japan). *Terra Nova*, 9:33–37.

Rhazi, M., Desbrières, J., Tolaimate, A., Rinaudo, M., Vottero, P., Alagui, A. & El Meray, M. 2002. Influence of the nature of the metal ions on the complexation with chitosan. Application to the treatment of liquid waste. *Eur. Polym. J.*, 38:1523–1530.

Rhazi, M., Tolaimate, A., Rhazi, M., Desbriéres, J., Tolaimate, A., Rinaudo, M., Alagui, A. & Vottero, P. 2001. Contribution to the study of the complexation of copper by chitosan and oligomers. *Polymer (Guildf)*, 43:1267–1276.

Rinaudo, M. 2006. Chitin and chitosan: properties and applications. *Prog. Polym. Sci.*, 31:603–632.

Risgaard-Petersen, N., Langezaal, A. M., Ingvardsen, S., Schmid, M. C., Jetten, M. S. M., den Camp, H. J. M. O., Derksen, J. W. M., Piña-Ochoa, E., Eriksson, S. P., Nielsen, L. P., Revsbech, N. P., Cedhagen, T. & van der Zwaan, G. J. 2006. Evidence for complete denitrification in a benthic foraminifer. *Nature*, 443:93–96.

Ruthensteiner, B. 2008. Soft part 3D visualization by serial sectioning and computer reconstruction. *Zoosymposia*, 1:63–100.

Sigwart, J. D., Sumner-Rooney, L. H., Schwabe, E., Heß, M., Brennan, G. P. & Schrodl, M. 2014. A new sensory organ in 'primitive' molluscs (Polyplacophora: Lepidopleurida), and its context in the nervous system of chitons. *Front. Zool.*, 11:7.

Thalmann, H. & Bermudez, P. J. 1954. *Chitinosiphon*, a new genus of the Rhizamminidae. *Contrib. Cushman Found. Foram. Res.*, 5:53–54.

Travis, J. L. & Bowser, S. S. 1991. The motility of foraminifera. *In*: Lee, J. J. & Anderson, O. R. (ed.), Biology of Foraminifera. Academic Press, London. p. 91–155.

Trivedi, A., Mavi, P. S., Bhatt, D. & Kumar, A. 2016. Thiol reductive stress induces cellulose-anchored biofilm formation in *Mycobacterium tuberculosis*. *Nat. Commun.*, 7:1–15.

Tsuchiya, M., Toyofuku, T., Uematsu, K., Bruchert, V., Collen, J., Yamamoto, H. & Kitazato, H. 2015. Cytologic and genetic characteristics of endobiotic bacteria and kleptoplasts of *Virgulinella fragilis* (Foraminifera). *J. Eukaryot. Microbiol.*, 62:454–469.

Tsutsumi, Y., Koga, H., Qi, Z. D., Saito, T. & Isogai, A. 2014. Nanofibrillar chitin aerogels as renewable base catalysts. *Biomacromolecules*, 15:4314–4319.

Van der Zwaan, G. J., Duijnstee, I. A. P., den Dulk, M., Ernst, S. R., Jannink, N. T. & Kouwenhoven, T. J. 1999. Benthic foraminifers: proxies or problems? A review of paleocological concepts. *Earth Sci. Rev.*, 46:213–236.

Woehle, C., Roy, A., Glock, N., Wein, T., Weissenbach, J., Rosenstiel, P., Hiebenthal, C., Michels, J., Schonfeld, J. & Dagan, T. 2018. A novel eukaryotic denitrification pathway in foraminifera. *Curr. Biol.*, 28:2536–2543.

Woodward, R. B., Sondheimer, F., Taub, D., Heusler, K. & McLamore, W. M. 1952. The total synthesis of steroids. *J. Am. Chem. Soc.*, 74:4223–4251.

Wu, J., Qin, Z., Qu, L., Zhang, H., Deng, F. & Guo, M. 2019. Natural hydrogel in American lobster: a soft armor with high toughness and strength. *Acta Biomater.*, 88:102–110.

SUPPORTING INFORMATION

Additional supporting information may be found online in the Supporting Information section at the end of the article.

Figure S1. A scanning electron micrograph (A), optical micrographs (B, C) and phase contrast micrographs (D, E) of *Chilostomella ovoidea* collected from bathyal Sagami Bay.